ELSEVIER

Journal of Chromatography B, 711 (1998) 127–138

JOURNAL OF CHROMATOGRAPHY B

Separation of proteins and viruses using two-phase aqueous micellar systems

Chia-li Liu[a], Daniel T. Kamei[a], Jonathan A. King[b], Daniel I.C. Wang[a], Daniel Blankschtein[a,*]

[a]*Department of Chemical Engineering, Massachusetts Institute of Technology, Cambridge, MA 02139, USA*
[b]*Department of Biology, Massachusetts Institute of Technology, Cambridge, MA 02139, USA*

Abstract

We discuss the utilization of a novel two-phase aqueous nonionic micellar system for the purification and concentration of biomolecules, such as proteins and viruses, by liquid–liquid extraction. The nonionic surfactant *n*-decyl tetra(ethylene oxide), $C_{10}E_4$, phase separates in water into two coexisting aqueous micellar phases by increasing temperature. The mild interactions of the $C_{10}E_4$ nonionic surfactant with biomolecules, combined with the high water content of the two coexisting micellar phases, suggest the potential utility of two-phase aqueous $C_{10}E_4$ micellar systems for the purification and concentration of biomolecules. In this paper, we review our recent experimental and theoretical studies involving the partitioning of several water-soluble proteins, including cytochrome *c*, soybean trypsin inhibitor, ovalbumin, bovine serum albumin, and catalase, in the two-phase aqueous $C_{10}E_4$ micellar system. In addition, we present results of our preliminary experimental investigation on the partitioning of bacteriophages, including ϕX174, P22, and T4.

Keywords: Two-phase aqueous systems; Partitioning; Proteins; Bacteriophages

1. Introduction

There has recently been growing interest in the utilization of two-phase aqueous micellar systems for the separation or concentration of biomolecules such as proteins [1–13]. This novel separation methodology exploits the remarkable fact that some aqueous micellar systems, under appropriate solution conditions, can spontaneously separate into two water-based, yet immiscible, liquid phases [14–17] between which proteins and other biomolecules can distribute unevenly while maintaining their native conformations and biological activities. These micellar systems are therefore suitable for the purification and concentration of biomolecules using liquid–liquid extraction principles, with the attractive feature of being readily scaled-up for operation on an industrial scale.

We will begin with a brief overview of micelles and aqueous micellar solutions. Micelles are self-assembling aggregates composed of surfactant molecules. A surfactant molecule consists of two distinct chemical moieties: the hydrophilic, water-loving moiety and the hydrophobic, water-fearing moiety. Micelles are formed in such a manner that the hydrophobic moieties of surfactant molecules flock inside to form the micellar core in order to minimize the unfavourable contact with water, while the hydrophilic moieties remain on the periphery to maximize their contact with the aqueous environ-

*Corresponding author.

0378-4347/98/$19.00
PII: S0378-4347(98)00013-9

ment [18,19]. The formation of micelles represents a delicate balance of several intermolecular forces, including those of the van der Waals, steric, hydrophobic, and electrostatic types [19,20]. The resulting micelles are labile microstructures formed by the noncovalent binding of individual surfactant molecules, contrary to polymers, for example, which are formed by the covalent binding of individual monomers. Consequently, micellar shape and size, as well as the associated micellar solution properties, can be tuned in situ by varying solution conditions, such as surfactant concentration, temperature, and salt type and concentration [18,19]. In addition, the micelles in an aqueous solution do not necessarily have a uniform size, but, instead, may exhibit a broad size distribution which can also be controlled in situ by changing the solution conditions mentioned above [17].

At certain temperatures and surfactant concentrations, a homogeneous aqueous micellar solution composed of certain surfactants can separate into two macroscopic phases, one rich in micelles, and the other poor in micelles. Fig. 1 illustrates such a phase separation phenomenon induced by increasing temperature. The fact that the water content in each of the two coexisting micellar phases is high, typically about or above 90% by weight, suggests that two-phase aqueous micellar systems are ideal for handling and processing biomolecules. The conditions at which phase separation of micellar solutions occurs can be characterized by the coexistence curve on the temperature versus surfactant concentration phase diagram (see Figs. 2 and 3 for examples).

When using surfactants or micellar systems for processing biomolecules, the type of surfactant is of concern because certain surfactants, particularly those of the ionic (charged) variety, are known to bind to biomolecules, such as proteins, often inducing denaturation and loss of biological activity. Nonetheless, it has been found that nonionic (noncharged) surfactants do not bind to biomolecules to a significant extent and do not denature proteins [21–23]. Accordingly, two-phase aqueous micellar systems composed of nonionic surfactants can provide a mild and friendly environment to biomolecules. This feature, combined with the phase separation behav-

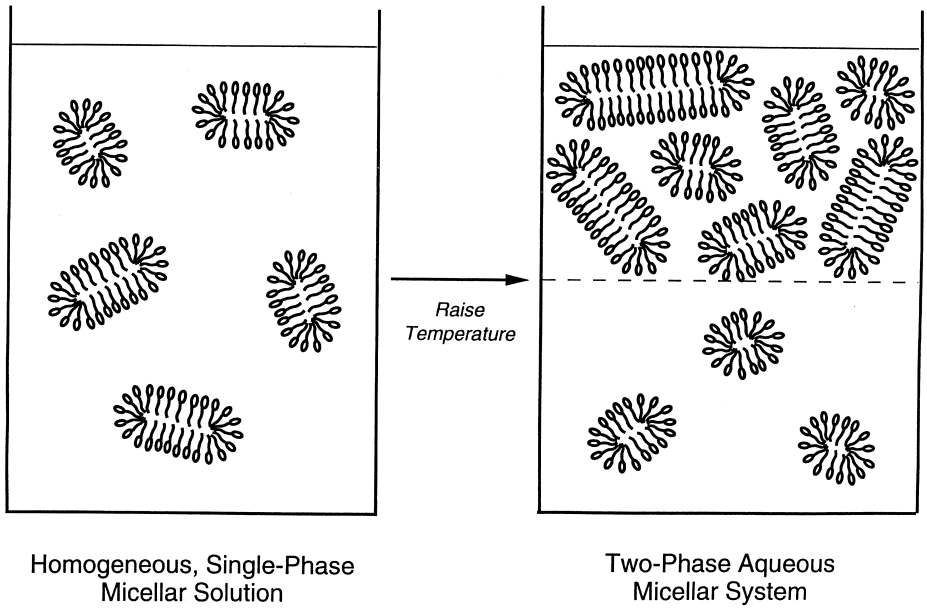

Fig. 1. Schematic illustration of phase separation of a micellar solution containing cylindrical micelles. A homogeneous, single-phase micellar solution may spontaneously separate into two micellar phases by changing solution conditions, for example, by increasing temperature in aqueous solutions composed of the nonionic surfactant *n*-decyl tetra(ethylene oxide) ($C_{10}E_4$). Both of the resulting coexisting phases contain cylindrical micelles but have different micellar concentrations. In addition, the micelles in the micelle-rich phase (top phase in the figure) are larger in size and greater in number than those in the micelle-poor phase (bottom phase in the figure).

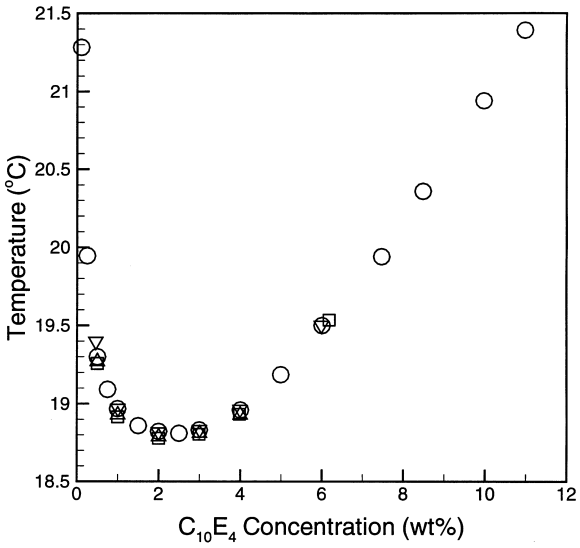

Fig. 2. Experimentally measured coexistence curves of aqueous $C_{10}E_4$ micellar solutions without protein (○) and with 0.25 g/l of cytochrome *c* (△), 0.5 g/l of ovalbumin (▽), and 0.5 g/l of catalase (□). The measurements were conducted using the cloud-point method. The typical error of the measured temperature is ±0.03°C.

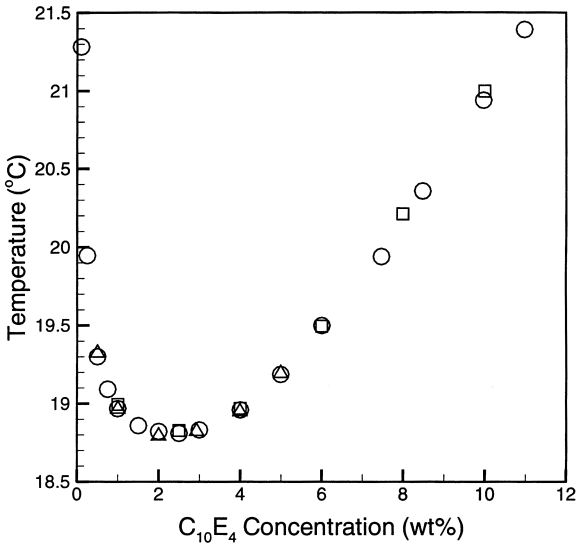

Fig. 3. Experimentally measured coexistence curves of aqueous $C_{10}E_4$ micellar solutions without bacteriophage (○), with 10^8 P22 particles per ml (△), and with 2×10^8 T4 particles per ml (□). The measurements were conducted using the cloud-point method. The typical error of the measured temperature is ±0.03°C.

iour and the high water content of the two coexisting micellar phases, suggests that two-phase aqueous micellar systems composed of nonionic surfactants are analogous to the more traditional two-phase aqueous nonionic polymer systems [24], and can therefore be utilized for the same purpose of partitioning and separating biomolecules.

When compared with the extensively studied two-phase aqueous polymer systems [24–30], two-phase aqueous micellar systems share many similarities with their polymer counterpart, but also offer several unique and desirable features (see Ref. [13] for schematic illustrations of these features):

1. For the simplest case, only a binary surfactant–water system is required to generate a two-phase aqueous micellar system, while the more complex ternary polymer 1–polymer 2–water or polymer–salt–water system is required to generate a two-phase aqueous polymer system.
2. The self-assembling, labile nature of micelles enables one to control and optimize the partitioning behaviour by tuning micellar characteristics, such as micellar shape and size. This can be accomplished by varying solution conditions, including temperature, surfactant concentration, and the addition of salts. On the other hand, the unchangeable identity of the polymers after their synthesis does not provide such flexibility.
3. The dual character of micelles, that is, their ability to simultaneously offer both hydrophobic and hydrophilic environments to solute species, allows the partitioning to be selective according to the hydrophobicity of biomolecules. Aqueous micellar systems have therefore been used for the extraction of hydrophobic materials, in general, and of hydrophobic biomolecules, in particular [1–6,8–11].
4. The partitioning can be made more selective by utilizing mixed micelles consisting of surfactant-type affinity ligands or charged surfactants mixed with the nonionic surfactant. By exploiting either the biospecific or electrostatic attractive interactions between the mixed micelles and the biomolecules, the desired biomolecules can be effectively concentrated in the micelle-rich phase of the two-phase aqueous mixed micellar system.

5. Removal of micelles from the desired biomolecules after partitioning can also be facilitated by exploiting the self-assembling character of micelles. For example, micelles can be disassembled into their constituent surfactant molecules, followed by filtration of the biomolecule–surfactant solution to remove the surfactant.

In view of the above, two-phase aqueous micellar systems provide an interesting alternative to two-phase aqueous polymer systems for partitioning or separating biomolecules using liquid–liquid extraction. It is therefore both practically interesting and fundamentally important to investigate how biomolecules partition between the two coexisting micellar phases, as well as to identify the major underlying driving forces responsible for the observed partitioning behaviour of biomolecules in two-phase aqueous micellar systems.

Our studies so far have focused on the partitioning behaviour of water-soluble biomolecules, including proteins and viruses, in two-phase aqueous micellar systems. The biomolecule partition coefficient, K, defined as the ratio of the biomolecule concentration in the top phase (C_t) to that in the bottom phase (C_b), that is, $K=C_t/C_b$, was used to quantify the biomolecule partitioning behaviour. In one of our previous publications [7], we presented a theoretical formulation to describe and predict the partitioning of water-soluble (hydrophilic) proteins in two-phase aqueous micellar systems containing nonionic micelles. The theory was based on the assumption that excluded-volume interactions between the globular hydrophilic proteins and the nonionic micelles play the dominant role in determining the experimentally observed partitioning behaviour. The excluded-volume formulation incorporates (i) the self-assembling character of micelles, which enables them to grow into long, cylindrical microstructures by varying temperature and/or surfactant concentration, and (ii) a broad distribution of micellar sizes associated with the cylindrical micelles. The theoretically predicted protein partition coefficient was compared with that measured experimentally for the hydrophilic protein, ovalbumin. In the two-phase aqueous micellar system composed of the nonionic surfactant *n*-decyl tetra(ethylene oxide) ($C_{10}E_4$), which tends to form cylindrical micelles [17,31,32], the theory was found to be in good agreement with the experiments. In addition, a comprehensive comparison of the similarities and differences in protein partitioning in two-phase aqueous micellar and polymer systems was presented.

In more recent publications [12,13], we presented extensive experimental data on the partitioning behaviour of several water-soluble proteins of various sizes, including cytochrome *c*, soybean trypsin inhibitor, ovalbumin, bovine serum albumin, and catalase (in the order of increasing size), in the two-phase aqueous $C_{10}E_4$ micellar system. In addition, partitioning results for cytochrome *c*, ovalbumin, and catalase in the two-phase aqueous micellar system composed of the zwitterionic (noncharged) surfactant dioctanoyl phosphatidylcholine (C_8-lecithin) were presented. Both surfactants were found to form cylindrical micelles in aqueous solutions [17,31,32]. Good agreement was found between the experimental protein partition coefficients and the theoretical values predicted in the context of the excluded-volume theory. This clearly indicates that excluded-volume interactions between the noncharged (nonionic or zwitterionic) cylindrical micelles and the globular water-soluble proteins are the dominant driving force for the observed protein partitioning behaviour. Furthermore, according to the excluded-volume theory, biomolecules having sizes larger than typical proteins should exhibit more extreme partitioning behaviour in the two-phase aqueous micellar systems examined. This prediction, based on the excluded-volume theory, prompted our recent investigation of viral partitioning. The preliminary results of this investigation are presented for the first time in this paper.

Viral particles have radii ranging from about 100 Å to 2000 Å, and are therefore larger than typical proteins. In addition to testing the range of validity and applicability of the excluded-volume theoretical formulation for larger biomolecules, partitioning of viral particles may aid in the implementation of two-phase aqueous micellar systems as a novel separation tool for the purification and concentration of viruses. This is potentially useful in many practical applications, such as diagnostics, vaccine production, and gene therapy. In the preliminary studies on viral partitioning, bacteriophages with protein exteriors, including ϕX174, P22, and T4 (in the

order of increasing size), were used as model viral particles. The major reasons for choosing bacteriophages for the partitioning studies were (i) availability, (ii) safety, related to their being noninfective to humans, and (iii) accurate concentration determination using the plaque assay.

Below, we review our recent experimental and theoretical work on the partitioning of water-soluble proteins in the two-phase aqueous $C_{10}E_4$ micellar system. We will also present for the first time our preliminary partitioning results for bacteriophages in the two-phase aqueous $C_{10}E_4$ micellar system. The experimentally observed viral partitioning behaviour is then compared and contrasted with that of the water-soluble proteins examined, as well as with the theoretical predictions based on the excluded-volume theory.

2. Experimental

2.1. Materials

Homogeneous *n*-decyl tetra(ethylene oxide) ($C_{10}E_4$) (lot no. 1006) was purchased from Nikko Chemicals (Tokyo, Japan). The water-soluble proteins cytochrome *c*, soybean trypsin inhibitor, ovalbumin, bovine serum albumin, and catalase were obtained from Sigma Chemicals (St. Louis, MO, USA). The bacteriophage ϕX174 type am(E)W4 and its host bacterium, *Escherichia coli* BAF5, were provided by Professor Bentley Fane in the Department of Biological Science at the University of Arkansas. Bacteriophages P22 and T4-D (wild type), as well as the P22 host bacterium, *Salmonella typhimurium* strain 7155, were obtained from Professor Jonathan King's laboratory. The host bacterium of T4-D, *Escherichia coli* B40, was provided by Professor Edward Goldberg in the Department of Microbiology at Tufts University. The bacteriophages were provided in aqueous solutions with concentrations of about 10^{11} viral particles per ml. All these materials were used as received.

All solutions were prepared using deionized water processed by a Milli-Q ion-exchange system, and were buffered at pH 7.0 with 10 m*M* citric acid and 20 m*M* disodium phosphate (McIlvaine buffer). Solutions also contained 0.02% sodium azide to prevent bacterial growth.

2.2. Experimental procedures

2.2.1. Coexistence curve measurement

The coexistence curve (described in Section 1) of the aqueous $C_{10}E_4$ system, with or without added biomolecules (water-soluble proteins or bacteriophages), was determined using the cloud-point method (see Refs. [7,12,13,17] for complete details). In this method, for a given surfactant concentration, the temperature at which a given surfactant solution becomes turbid and cloudy, that is, the cloud-point temperature (T_{cloud}), is identified, since such behaviour signals the onset of phase separation. Each reported cloud-point temperature results from taking an arithmetic average of at least 6 experimental T_{cloud} values. It should also be noted that the concentrations of biomolecules in the aqueous $C_{10}E_4$ solutions were chosen to be the same as those used in the partitioning experiments in order to probe the effect of biomolecule concentration on the phase separation behaviour at the actual partitioning conditions.

2.2.2. Partitioning of water-soluble proteins

To measure the protein partition coefficient, K_p, buffered solutions containing known concentrations of $C_{10}E_4$ and of the water-soluble protein of interest were prepared, and subsequently allowed to equilibrate at a fixed temperature for at least 6 h to ensure that phase separation equilibrium was attained. The $C_{10}E_4$ concentration was selected to correspond to that of the mid-point of the horizontal tie line which was drawn across the coexistence curve at the temperature of interest. This was done to ensure that the volumes of the two coexisting micellar phases were approximately the same. An equal volume ratio, that is, $V_{top}/V_{bot} \approx 1$, was chosen to conserve the amount of protein used in each experiment, since approximately 1 ml of each phase was required for assaying purposes. In addition, instead of maintaining a constant overall $C_{10}E_4$ concentration for the different temperatures investigated, the volume ratio was the operating parameter held constant in the experiments. From each phase-separated solution, the two phases were then withdrawn with great care

using syringe and needle sets, and the protein concentration in each phase was determined using UV absorbance measurements on a Shimadzu UV 160U spectrophotometer. For complete details, see Refs. [12,13].

2.2.3. Partitioning of bacteriophages

For the partitioning experiments involving bacteriophages, the plaque assay was utilized to determine the virus concentrations. This assay was conducted by (i) diluting the virus solution to an appropriate concentration, (ii) incubating a fixed volume of the diluted virus solution with the host bacterium and nutrients on an agar plate overnight, and (iii) counting the number of plaques generated on the plate. The virus concentration in the original solution can be calculated from the number of plaques and the dilutions conducted. Since one plaque on the agar plate represents one infective viral particle, the plaque assay determines the concentration of the viral particles which are biologically active and infectious.

Before conducting the partitioning of bacteriophages in the $C_{10}E_4$ micellar system, the stability of the virus in the micellar solution was tested at room temperature (which is comparable to the temperature range for the partitioning experiments). The purpose of this test was to examine the stability and viability of the virus in the micellar solution, and to ensure that the presence of the surfactant would not interfere with the virus concentration determination using the plaque assay. The virus stability was quantified in terms of the variation of the virus concentration (as determined by the plaque assay) with time at various solution conditions, including the McIlvaine buffer alone and 10 wt% of $C_{10}E_4$ in McIlvaine buffer. This $C_{10}E_4$ concentration was selected because it is the highest surfactant concentration utilized in the partitioning experiments. Results of the stability test indicated that, in order to attain the maximum accuracy in the virus concentration determination, the bacteriophages ϕX174 and T4 should be assayed within 8 h after being exposed to $C_{10}E_4$, while P22 could be accurately assayed even after the virus is exposed to $C_{10}E_4$ for one day. Taking into consideration the time needed for conducting the plaque assay, which is about 3–4 h, the maximum partitioning time allotted for ϕX174 and T4 was about 4–5 h, while that alloted for P22 was about 16 h.

To measure the virus partition coefficient, K_v, buffered solutions containing known concentrations of $C_{10}E_4$ were prepared, followed by the addition of a concentrated virus solution to generate a final virus concentration of about 10^8 viral particles per ml. To be consistent with the protein partitioning experiments, the $C_{10}E_4$ concentration in each of the virus partitioning experiments was also selected to ensure that the volumes of the two coexisting micellar phases were approximately the same. The solutions were then well mixed by vortexing, and subsequently allowed to equilibrate at a fixed temperature to allow phase separation to occur. As stressed above, the partitioning experiments were conducted for about 4 h in the case of ϕX174 and T4, and for about 16 h in the case of P22. The resulting two coexisting micellar phases were then withdrawn with great care using syringe and needle sets, and the virus concentration in each phase was determined using the plaque assay.

3. Results and discussion

3.1. Partitioning of proteins

Fig. 2 shows the experimentally measured coexistence curves of aqueous $C_{10}E_4$ micellar solutions without protein, and with 0.25 g/l cytochrome *c*, 0.5 g/l ovalbumin, and 0.5 g/l catalase in McIlvaine buffer at pH 7. The measured cloud-point temperatures were reproducible to within 0.03°C. The coexistence curve delineates the boundary which separates the conditions at which the micellar solution exhibits different phase behaviour. Specifically, the region within the coexistence curve is the two-phase region, denoting conditions at which the micellar solution separates spontaneously into two macroscopic phases, while the region outside the coexistence curve is the one-phase region, denoting conditions at which the micellar solution exists as a single, homogeneous phase. This figure indicates that phase separation of the aqueous $C_{10}E_4$ micellar solution occurs above 18.8°C, and therefore, the partitioning experiments in this micellar system have to be conducted above this minimum temperature,

which is referred to as the critical temperature (T_c). In addition, Fig. 2 also shows that, in the range of $C_{10}E_4$ concentrations examined, the phase separation behaviour of the micellar solution is not affected by the presence of the added proteins. This finding is significant, since it indicates that the description of the micellar solution phase separation phenomenon is independent of, and can therefore be decoupled from, the protein partitioning phenomenon. This important finding was utilized in the development of the excluded-volume theoretical formulation [7].

Fig. 4 shows the experimentally measured partition coefficients, K_p, of cytochrome *c*, ovalbumin, and catalase as a function of the partitioning temperature in the range of 18.8 to 21.2°C in the two-phase aqueous $C_{10}E_4$ micellar system at pH 7. The overall protein concentrations were the same as those utilized in the coexistence curve measurements, that is, 0.25 g/l cytochrome *c*, 0.5 g/l ovalbumin, and 0.5 g/l catalase, respectively. The fact that $K_p<1$ for all three proteins clearly indicates that these water-soluble proteins partition preferentially into the bottom, micelle-poor phase of the two-phase aqueous $C_{10}E_4$ micellar system. In addition, as the temperature T increases, or more specifically, as the difference between T and the critical temperature $T_c=18.8$°C, that is, $(T-T_c)$, increases, K_p decreases and deviates further from unity for the three proteins. Furthermore, at a fixed temperature, the K_p values of these proteins are in the order of K_p (catalase)$<K_p$ (ovalbumin)$<K_p$ (cytochrome *c*)<1, which is opposite to the order of their sizes [catalase (M_r of 232 000 Da)$>$ovalbumin (M_r of 44 000 Da)$>$ cytochrome *c* (M_r of 12 400 Da)]. This clearly indicates that larger proteins tend to partition more extremely into the bottom, micelle-poor phase.

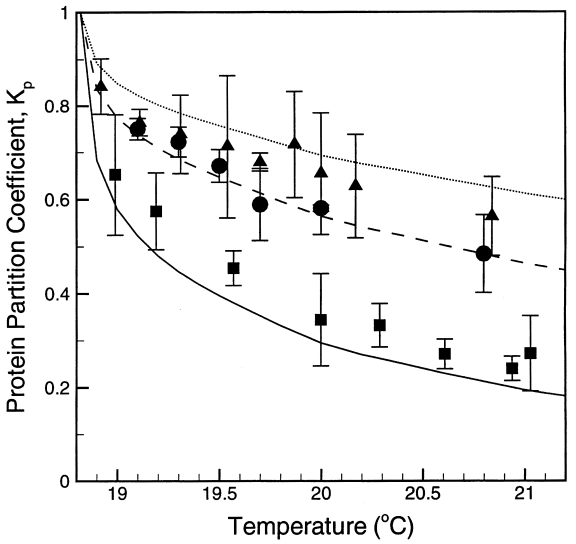

Fig. 4. Experimentally measured partition coefficients, K_p, of cytochrome *c* (▲), ovalbumin (●), and catalase (■) at different temperatures in the two-phase aqueous $C_{10}E_4$ micellar system. The error bars represent 95% confidence limits of the measurements. Also shown are the predicted K_p's of cytochrome *c* (· · ·), ovalbumin (- - -), and catalase (———) as a function of temperature (see Eq. (1)).

The observations above indicate that water-soluble proteins are driven into the phase which has a larger free volume, that is, into the bottom, micelle-poor phase. This tendency is stronger as $(T-T_c)$ increases, that is, as the difference in the micellar concentrations (or the volume fractions occupied by micelles) of the two coexisting micellar phases becomes more pronounced, as shown in the coexistence curve (see Fig. 2). This tendency is also stronger as the size of the water-soluble proteins increases. In other words, these observations are all consistent with the notion that excluded-volume interactions between the water-soluble proteins and the noncharged $C_{10}E_4$ micelles play the dominant role in the observed protein partitioning behaviour.

Based on the experimental findings described above, we formulated a theoretical description of the protein partitioning behaviour in which only excluded-volume interactions between noncharged micelles and proteins operate. More specifically, we assumed that the water-soluble proteins and the $C_{10}E_4$ nonionic micelles behave as mutually nonpenetrable hard objects interacting through short-ranged, repulsive, excluded-volume interactions. Results of other experimental and theoretical studies [17,32,31] have shown that $C_{10}E_4$ tends to form cylindrical micelles with polydisperse sizes in aqueous solutions, and that the $C_{10}E_4$ micelles are rigid as viewed on the scale of a typical protein molecule [7]. Consequently, we assumed [7] that, in the aqueous protein–$C_{10}E_4$ micellar system, the cylindrical $C_{10}E_4$ micelles can be modeled as polydisperse, hard spherocylinders, while the globular water-soluble proteins can be modeled as monodisperse, hard

spheres. The resulting protein partition coefficient, K_p, is given by (for complete details, see Ref. [7])

$$K_p = \exp\left[-(\phi_t - \phi_b)\left(1 + \frac{R_p}{R_0}\right)^2 \right] \quad (1)$$

where ϕ_t and ϕ_b are the volume fractions of micelles in the top and bottom phases, respectively, R_p is the protein hydrodynamic radius, and R_0 is the cross-sectional radius of the cylindrical micelles. Eq. (1) predicts that K_p depends on two factors: (i) the difference in the micellar concentrations of the two coexisting micellar phases, that is, the $(\phi_t - \phi_b)$ term, and (ii) the relative sizes of micelles and proteins, as reflected in the R_p/R_0 ratio. The $(\phi_t - \phi_b)$ term is a function of temperature, and can be obtained from the coexistence curve shown in Fig. 2. The radii R_0 and R_p are determined by the chemical structures of $C_{10}E_4$ and the protein, respectively. Accordingly, the theory contains no adjustable parameters.

In order to predict K_p as a function of temperature using Eq. (1), the values of R_0, R_p, as well as that of $(\phi_t - \phi_b)$ as a function of temperature are needed. In general, R_0 is approximately equal to the length of the surfactant molecule. Calculations based on a molecular model of micellization [31,33,34] yield $R_0 \approx 21$ Å for $C_{10}E_4$. The hydrodynamic radii, R_p, of cytochrome *c*, ovalbumin, and catalase are 19, 29, and 52 Å, respectively [29]. The $(\phi_t - \phi_b)$ values at various temperatures can be obtained from the coexistence curve shown in Fig. 2. Specifically, the ϕ_t and ϕ_b values at a certain temperature correspond to the surfactant concentrations at which the horizontal tie line at that temperature intersects the concentrated and dilute branches of the coexistence curve, respectively. Recall that the top phase in the two-phase aqueous $C_{10}E_4$ micellar system is micelle-rich, while the bottom phase is micelle-poor.

Fig. 4 shows K_p as a function of temperature for cytochrome *c*, ovalbumin, and catalase predicted using Eq. (1) with the R_p, R_0 and $(\phi_t - \phi_b)$ values obtained as described above. As can be seen, there is reasonable agreement between the experimentally measured and the theoretically predicted K_p values, indicating that the universal, nonspecific, excluded-volume description captures fairly well the observed protein partitioning behaviour.

An alternative illuminating way to compare the theoretical and experimental K_p values is to plot K_p as a function of the R_p/R_0 ratio at a fixed temperature, or, equivalently, at a fixed $(\phi_t - \phi_b)$ value. Fig. 5 shows the predicted K_p values as a function of R_p/R_0, along with the experimental K_p values of cytochrome *c*, soybean trypsin inhibitor, ovalbumin, bovine serum albumin, and catalase at 21°C, which corresponds to $(\phi_t - \phi_b) \approx 10\%$. The hydrodynamic radii of soybean trypsin inhibitor and bovine serum albumin are 22 and 36 Å, respectively [35]. Once again, there is reasonable agreement between the theoretical predictions and the experimental observations. Fig. 5 also indicates that K_p decreases as R_p increases relative to R_0, with the predicted K_p values becoming vanishingly small when $R_p/R_0 > 5$, that is, when $R_p > 100$ Å. As long as excluded-volume interactions are dominant, this suggests that water-soluble biomolecules with $R > 100$ Å, such as viruses or cells, should exhibit a very extreme partitioning behaviour in the two-phase aqueous $C_{10}E_4$ micellar system. Results of preliminary experimental virus

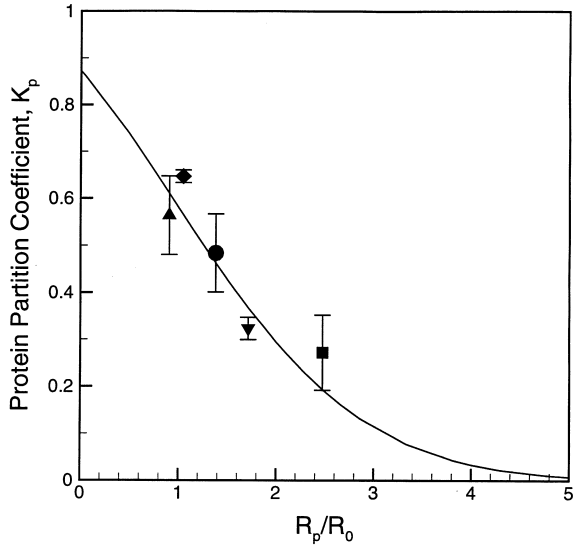

Fig. 5. Experimentally measured K_p values of cytochrome *c* (▲, $R_p = 19$ Å), soybean trypsin inhibitor (♦, $R_p = 22$ Å), ovalbumin (●, $R_p = 29$ Å), bovine serum albumin (▼, $R_p = 36$ Å), and catalase (■, $R_p = 52$ Å), as a function of the R_p/R_0 ratio in the two-phase aqueous $C_{10}E_4$ micellar system at 21°C, where $R_0 = 21$ Å is the cross-sectional radius of the $C_{10}E_4$ cylindrical micelles. The error bars represent 95% confidence limits of the measurements. The line represents the predicted K_p values calculated using Eq. (1), with $(\phi_t - \phi_b) = 10\%$ at 21°C.

partitioning studies in the two-phase aqueous $C_{10}E_4$ micellar system are presented next.

3.2. Partitioning of viruses

Fig. 3 shows the experimentally measured coexistence curves of aqueous $C_{10}E_4$ micellar solutions without bacteriophages and with 10^8 P22 particles per ml and 2×10^8 T4 particles per ml in McIlvaine buffer of pH 7. Similar to Fig. 2, Fig. 3 indicates that the added bacteriophages have a negligible effect on the phase separation behaviour of the aqueous $C_{10}E_4$ micellar solution. Although not shown in Fig. 3, the effect of added ϕX174 on the phase separation behaviour was also found to be negligible.

Fig. 6 shows the experimentally measured partition coefficient, K_v, of ϕX174 as a function of temperature in the two-phase aqueous $C_{10}E_4$ micellar system at pH 7, as an illustration of the bacteriophage partitioning results. Note that the scale of the *y*-axis is logarithmic. Also shown in Fig. 6 are the K_p values of ovalbumin (without error bars, since they are not visible in a logarithmic scale) over the same temperature range for comparison purposes. The fact that $K_v < 1$ shows the tendency of ϕX174 to partition preferentially into the bottom, micelle-poor phase. In addition, K_v of ϕX174 deviates increasingly from unity as the temperature increases, that is, as $(T-T_c)$ increases. These phenomena are qualitatively similar to those observed for the partitioning of water-soluble proteins. However, the K_v values of ϕX174 are significantly lower than those of the proteins examined earlier, with K_v of ϕX174 reaching about 2×10^{-3} at 21°C, while the K_p values are essentially of order unity. This indicates that much more extreme partitioning of viruses can indeed be attained. In fact, ϕX174 is the smallest among the three bacteriophages examined in the virus partitioning studies. Specifically, ϕX174 is icosahedral in shape, and hence, can be modeled as a sphere with a radius of 125 Å [36], which is larger than that of typical proteins with hydrodynamic radii ranging between 20 to 60 Å. Consequently, the more extreme partitioning behaviour exhibited by ϕX174 is qualitatively consistent with the excluded-volume theoretical predictions shown in Fig. 5. In fact, the excluded-volume theoretical formulation leading to Eq. (1) was also used to predict the partitioning behaviour of ϕX174 under the assumption that this formulation is still valid in the virus case. Substituting $R_v = 125$ Å for ϕX174, and following the same procedures described in the previous section, K_v of ϕX174 was predicted as a function of temperature and is also shown in Fig. 6. As can be seen, the predicted ϕX174 K_v values agree well with the experimentally measured K_v values (within experimental error) in the temperature range examined. This indicates that the excluded-volume theoretical description is also fairly accurate in describing the partitioning behaviour of small viruses.

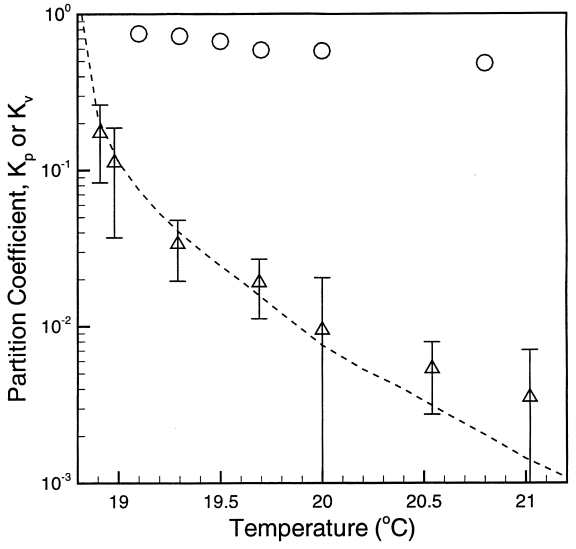

Fig. 6. Experimentally measured partition coefficient, K_v, of the bacteriophage ϕX174 (△) at different temperatures in the two-phase aqueous $C_{10}E_4$ micellar system. The error bars represent 95% confidence limits of the measurements. The partition coefficient K_p of ovalbumin (○) at different temperatures is also shown for comparison purposes. Note that the error bars of the ovalbumin data are not included in this figure because they are not visible in the logarithmic scale used. The dashed line represents the predicted K_v values of ϕX174 as a function of temperature calculated from Eq. (1).

In order to examine how K_v varies with the size of the virus, in Fig. 7, K_v is plotted as a function of the virus radius, R_v, for the three bacteriophages examined, ϕX174, P22, and T4, in the two-phase aqueous $C_{10}E_4$ micellar system at pH 7 and 21°C (corresponding to $(\phi_t - \phi_b) \approx 10\%$). The P22 particles are also icosahedral in shape, and hence can be viewed and modeled as spheres having a radius of

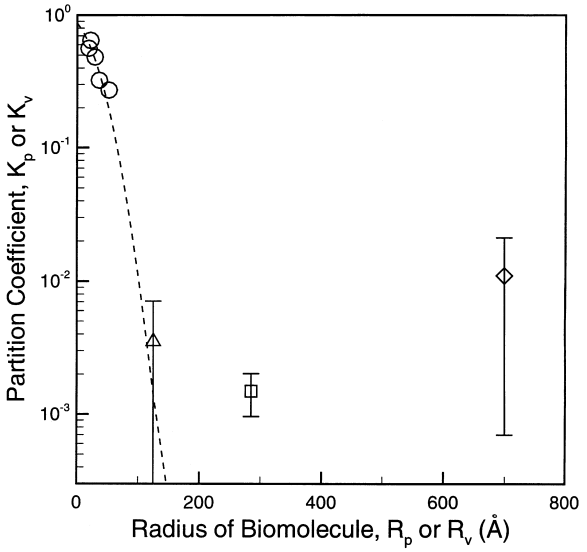

Fig. 7. Experimentally measured K_v values of ϕX174 (△, R_v = 125 Å), P22 (□, R_v = 285 Å), and T4 (◇, $R_v \approx 700$ Å), plotted as a function of the radius of the virus, R_v, in the two-phase aqueous $C_{10}E_4$ micellar system at 21°C. The error bars represent 95% confidence limits of the measurements. The K_p values of the water-soluble proteins, including cytochrome *c*, soybean trypsin inhibitor, ovalbumin, bovine serum albumin, and catalase (in the order of increasing R_p) (○) at 21°C are also shown as a function of the protein radius, R_p, for comparison purposes. The dashed line represents the predicted K_p or K_v values calculated from Eq. (1), with $(\phi_t - \phi_b) = 10\%$ at 21°C.

285 Å [37]. The T4 particles are rod-like [38], and can be modeled as effective spheres having a radius of about 700 Å [39]. The K_p values of the five water-soluble proteins shown in Fig. 5 are also included in Fig. 7 for comparison purposes. As shown in Fig. 7, the average K_v values range between 10^{-3} and 10^{-2}, which are much lower than all the reported K_p values. However, the measured K_v values of these three bacteriophages are very similar, contrary to the prediction of the excluded-volume theory, which indicates that K_v should continue to decrease as the virus radius, R_v, increases.

Also shown in Fig. 7 are the predicted K_v values calculated from Eq. (1) using $(\phi_t - \phi_b) = 10\%$, $R_0 =$ 21 Å, and the appropriate R_v values for the ϕX174, P22, and T4 viral particles. The predicted *K*'s (K_p or K_v) agree reasonably well with the experimental data for all the proteins examined and for ϕX174. On the other hand, for the larger bacteriophages P22 and T4, the predicted K_v's are much lower than the experimental ones. Specifically, the predicted K_v values at this $(\phi_t - \phi_b)$ value are 10^{-13} and 10^{-70} for P22 and T4, respectively! Clearly, the excluded-volume theory severely overpredicts the viral partitioning behaviour obtained for the two larger viruses, with the disagreement between theory and experiment becoming more pronounced as the size of the virus increases. Two possible scenarios can be put forward to rationalize why the excluded-volume theory, which worked reasonably well for the smaller biomolecules including the five proteins examined and the bacteriophage ϕX174, does not correctly predict the partitioning behaviour of the larger viruses. Specifically,

1. Attractive interactions, which are not accounted for in the excluded-volume theory, may exist between micelles and viral particles (particularly the large bacteriophages P22 and T4) in addition to the repulsive, excluded-volume interactions. Such nonuniversal, attractive interactions may be induced by the tailspikes of P22 particles or the tail fibers of T4 particles. The tailspikes or tail fibers of these viruses, which interact with the bacterial membrane during viral infection, may be able to interact with micelles as well, since micelles are similar to the bacterial membrane in structure. These additional attractive interactions would result in higher virus concentrations in the top, $C_{10}E_4$ micelle-rich phase, which, in turn, would yield higher K_v values than predicted by the excluded-volume theory.
2. The observed viral partitioning behaviour may not reflect the true thermodynamic equilibrium condition which is predicted by Eq. (1). Equilibrium may not be attained because the mass transfer of the larger viral particles between the two coexisting micellar phases may be hindered by their low diffusivities and the high viscosity of the top, $C_{10}E_4$ micelle-rich phase. Another possibility is that small domains having the same micellar and virus concentrations as the macroscopic bottom, micelle-poor phase may be entrained in the macroscopic top, micelle-rich phase. In both cases, a larger than predicted number of viral

particles would remain in the top phase, thus yielding less extreme K_v values.

Studies aimed at investigating these two scenarios are in progress.

It should be kept in mind that, although the observed viral partitioning behaviour for P22 and T4 is not as extreme as that predicted by the excluded-volume theory, the difference between the observed K_p and K_v values is quite large, about two orders of magnitude. Such a large difference in the K_p and K_v values suggests that one should be able to achieve efficient separation of viruses from proteins using two-phase aqueous micellar systems. Work aimed at investigating this interesting possibility, which has clear practical ramifications, is in progress.

4. Conclusions

We have reviewed our experimental and theoretical work on the partitioning of water-soluble proteins, as well as presented our new preliminary experimental results on the partitioning of bacteriophages, in the two-phase aqueous $C_{10}E_4$ micellar system. For protein partitioning, the good agreement between the theoretically predicted and experimental K_p values indicates that excluded-volume interactions between the nonionic micelles and the proteins play the dominant role in the observed partitioning behaviour of water-soluble proteins. The bacteriophages examined were found to partition much more extremely than the proteins into the bottom, micelle-poor phase of the two-phase aqueous $C_{10}E_4$ micellar system. Specifically, the measured K_v values are two orders of magnitude lower than the measured K_p values. The excluded-volume theory, which is able to successfully describe the partitioning behaviour of the water-soluble proteins examined and of the smaller bacteriophage ϕX174, significantly overpredicts the partitioning behaviour of the larger bacteriophages P22 and T4. A thorough investigation is under way to elucidate the reasons for this overprediction.

The work presented in this paper clearly demonstrates that two-phase aqueous micellar systems are a promising new separation method for the purification and concentration of biomolecules, including proteins and viruses. Indeed, with the high water content of both phases, the nondenaturing nature of nonionic surfactants, and the convenience associated with a liquid–liquid extraction type operation, two-phase aqueous micellar systems are potentially useful for the separation, purification, and concentration of biomolecules on an industrial scale. More studies will be conducted to improve the separation efficiencies of two-phase aqueous micellar systems, as well as to investigate the partitioning behaviour of biomolecules other than proteins and viruses in these fascinating systems.

Acknowledgements

The authors would like to thank Cameron Haase-Pettingell and Barrie Greene in the Department of Biology at M.I.T. for offering technical instruction in the bacteriophage experiments and useful comments on virology. The authors would also like to thank Professor Bentley Fane in the Department of Biological Science at the University of Arkansas, and Professor Edward Goldberg in the Department of Microbiology at Tufts University for kindly providing the viruses used in the partitioning experiments. The authors would also like to acknowledge Per-Åke Albertsson, Donald Brooks, Göte Johansson, Maria-Regina Kula, Folke Tjerneld, and Harry Walter for illuminating discussions on two-phase aqueous separations. Discussions with Jill Myers and Cyrus Karkaria from Biogen Inc. have also been helpful and are greatly appreciated. This research was supported in part by the Biotechnology Process Engineering Center (BPEC) by NSF under the cooperative agreement EEC-880-3014 at M.I.T. and Biogen Inc. D.T. Kamei is grateful for the financial support from the Department of Defense, National Defense Science and Engineering Graduate Fellowship.

References

[1] C. Bordier, J. Biol. Chem. 256 (1981) 1604–1607.
[2] J.G. Pryde, Trends Biochem. Sci. 11 (1986) 160–163.
[3] J.G. Pryde, J.H. Phillips, Biochem. J. 233 (1986) 525–533.

[4] C. Holm, G. Fredrikson, P. Belfrage, J. Biol. Chem. 261 (1986) 15659–15661.
[5] R.A. Ramelmeier, G.C. Terstappen, M.-R. Kula, Bioseparation 2 (1991) 315–324.
[6] T. Saitoh, W.L. Hinze, Anal. Chem. 63 (1991) 2520–2525.
[7] Y.J. Nikas, C.-L. Liu, T. Srivastava, N.L. Abbott, D. Blankschtein, Macromolecules 25 (1992) 4797–4806.
[8] G.C. Terstappen, R.A. Ramelmeier, M.-R. Kula, J. Biotechnol. 28 (1993) 263–275.
[9] W.L. Hinze, E. Pramauro, Crit. Rev. Anal. Chem. 24 (1993) 133–177.
[10] A. Sánchez-Ferrer, R. Bru, F. García-Carmona, Crit. Rev. Biochem. Mol. Biol. 29 (1994) 275–313.
[11] T. Saitoh, H. Tani, T. Kamidate, H. Watanabe, Trends Anal. Chem. 14 (1995) 213–217.
[12] C.-L. Liu, Y.J. Nikas, D. Blankschtein, AIChE J. 41 (1995) 991–995.
[13] C.-L. Liu, Y.J. Nikas, D. Blankschtein, Biotechnol. Bioeng. 52 (1996) 185–192.
[14] V. Degiorgio, in: V. Degiorgio, M. Corti (Eds.), Proceedings of the International School of Physics Enrico Fermi-Physics of Amphiphiles: Micelles, Vesicles and Microemulsions, July 1983, North-Holland Physics Publishing, The Netherlands, 1985, pp. 303–335.
[15] J.C. Lang, in: V. Degiorgio, M. Corti (Eds.), Proceedings of the International School of Physics Enrico Fermi-Physics of Amphiphiles: Micelles, Vesicles and Microemulsions, July 1983, North-Holland Physics Publishing, The Netherlands, 1985, pp. 336–375.
[16] K.L. Mittal, B. Lindman (Eds.), Surfactants in Solution, Vols. 1–4, Plenum, New York and London, 1984.
[17] D. Blankschtein, G.M. Thurston, G.B. Benedek, J. Chem. Phys. 85 (1986) 7268–7288.
[18] Y. Chevalier, T. Zemb, Rep. Prog. Phys. 53 (1990) 279–371.
[19] C. Tanford, The Hydrophobic Effect: Formation of Micelles and Biological Membranes, Wiley, New York, 1980.
[20] J.N. Israelachvili, Intermolecular and Surface Forces, Academic, London and San Diego, 2nd ed., 1991.
[21] A. Helenius, K. Simons, J. Biol. Chem. 247 (1972) 3656–3661.
[22] S. Makino, J.A. Reynolds, C. Tanford, J. Biol. Chem. 248 (1973) 4926–4932.
[23] S. Makino, Adv. Biophys. 12 (1979) 131–184.
[24] P.-Å. Albertsson, Partition of Cell Particles and Macromolecules, 3rd ed., Wiley-Interscience, New York, 1986.
[25] H. Walter, D.E. Brooks, D. Fisher (Eds.), Partitioning in Aqueous Two-Phase Systems: Theory, Methods, Uses, and Applications to Biotechnology, Academic, Orlando, 1985.
[26] D. Fisher, I.A. Sutherland (Eds.), Separations Using Aqueous Phase Systems, Plenum, New York, 1987.
[27] N.L. Abbott, D. Blankschtein, T.A. Hatton, Bioseparation 1 (1990) 191–225.
[28] N.L. Abbott, D. Blankschtein, T.A. Hatton, Macromolecules 24 (1991) 4334–4348.
[29] N.L. Abbott, D. Blankschtein, T.A. Hatton, Macromolecules 25 (1992) 3917–3931.
[30] H. Walter, G. Johansson, D.E. Brooks, Anal. Biochem. 197 (1991) 1–18.
[31] S. Puvvada, D. Blankschtein, J. Chem. Phys. 92 (1990) 3710–3724.
[32] B. Lindman, H. Wennerström, J. Phys. Chem. 95 (1991) 6053–6054.
[33] A. Naor, S. Puvvada, D. Blankschtein, J. Phys. Chem. 96 (1992) 7830–7832.
[34] N.J. Zoeller, D. Blankschtein, Ind. Eng. Chem. Res. 34 (1995) 4150–4160.
[35] P.L. Dubin, J.M. Principi, J. Chromatogr. 479 (1989) 159–164.
[36] M. Hayashi, A. Aoyama, D.L. Richardson, Jr. M.N. Hayashi, in: R. Calendar (Ed.), The Bacteriophages, Vol. 2, Plenum Press, New York, 1988, pp. 1–71.
[37] W. Earnshaw, S. Casjens, S.C. Harrison, J. Mol. Biol. 104 (1976) 387–410.
[38] F.A. Eiserling, in: C.K. Mathers, E.M. Kutter, G. Mosig, P.B. Berget (Eds.), Bacteriophage T4, American Society for Microbiology, Washington, D.C., 1983, pp. 11–24.
[39] C. Liu, Ph.D. thesis, M.I.T., 1995.